ChemPubSoc Europe

DOI: 10.1002/chem.xxxxxxxxx

CHEMISTRY A European Journal Communication

A Spotlight on the Compatibility between XFEL and Ab Initio Structures of the Oxygen Evolving Complex in Photosystem II†

Daniele Narzi,[a,‡,*] Giuseppe Mattioli,[b,‡,*] Daniele Bovi,[c,d] and Leonardo Guidoni [d,*]

The Mn_4CaO_5 cluster of Photosystem II promotes a crucial step in the oxygenic photosynthesis, namely, the water splitting reaction. The structure of such cluster in the S_1 state of the Kok-Joliot's cycle has been recently resolved by femtosecond X-ray free electron laser (XFEL) measurements. However, the XFEL results are characterized by appreciable discrepancies with previous X-ray diffraction (XRD), as well as with S_1 models based on ab initio calculations. We provide here a unifying picture based on a combined set of DFT-based structures and molecular dynamics simulations of the S_0 and S_1 states. Our findings indicate that the XFEL results cannot be interpreted on the grounds of a single structure. A combination of two S_1 stable isomers together with a minority contribution of the S_0 state is necessary to reproduce XFEL results within 0.16 Å.

TOC: *Shedding light into the water-splitting cycle of Photosystem II: DFT calculations indicates that the recent XFEL structure of Photosystem II complex cannot be interpreted on the grounds of a single structure: two S_1 isomers may coexist together with a minority contribution of the S_0 state.*

Water oxidation occurring in the light reaction of the natural photosynthesis is catalyzed by the membrane complex Photosystem II (PSII) [1]. The water splitting reaction proceeds along the five S_0 - S_4 steps of the Kok-Joliot cycle [2,3] in which two water molecules are oxidized to molecular oxygen, four protons and four electron equivalents. The reaction takes place in the catalytic core of PSII consisting of the Mn_4CaO_5 cluster. The characterization of the structure, the energetics and the electronic state of each step of the catalytic cycle occurring in PSII is of central importance in order to understand its catalytic mechanism and to inspire the design of new materials suitable for artificial photosynthesis and solar fuel production [4–6]. Since the first XRD structures of PSII were resolved at 3.8 Å [7] and 3.5 Å [8] resolution, atomic details of the manganese cluster have been revealed at an increasing level of accuracy by further series of XAFS and XRD measurements. [9–12]. The last crystallographic structure of the S_1 state solved in 2015 [13] was obtained by using femtosecond XFEL pulses, which are expected to avoid radiation damage effects that may reduce Mn ions. However, the positions of the atoms belonging to the Mn_4CaO_5 cluster, particularly the μ-oxo O5 (see Fig. 1), are still matter of debate. In this respect several theoretical studies have been carried out in order to explain the unusually large Mn4-O5 bond length ($\sim$ 2.3 Å) found in the XFEL structure. Askerka *et al.* suggested that the residual discrepancy between XFEL and *ab initio* structures could be explained by an intrinsic uncertainty about the position of the O5 atom itself, still present at 1.95 Å resolution [14]. Moreover, contamination of the XFEL sample with the S_0 state of PSII cannot be excluded [14,15].

Indeed, μ-oxo oxygens in the Mn_4CaO_5 cluster are surrounded by electron-rich metal centers. Their positions, particularly in the case of O5 surrounded by four metal centers, can be poorly resolved by XFEL measurements. This hypothesis was also independently validated by Siegbahn [16] and Pantazis and coworkers [17] by means of DFT calculations, which suggested for the S_1 state an open cubane geometry with O5 bonded to Mn4, having the same protonation pattern predicted for the S_2 state (i.e., W2 present as hydroxyl and deprotonated O5). This suggestion was also in agreement with the experimental work of Dau and coworkers showing no change in the protonation state during the S_1 to S_2 transition [18]. However, an alternative S_1 structure bearing a water molecule instead of a hydroxyl in W2 was found to be consistent with the putative S_1 state. In this regard, Luber *et al.* suggested for the S_1 state the presence of the W2 molecule in the H_2O state [19], also more compatible with a Mn-O distance approaching 2.1 Å suggested by XFEL measurements. Concerning the oxidation states of the Mn ions in the S_1 state, these were predicted by theoretical studies to be consistent with the high-valent paradigm [16,17] (e.g. Mn1(III)Mn2(IV)Mn3(IV)Mn4(III) [20]) in agreement with those also suggested by Suga et al. [13]. In contrast, it was recently proposed that the atoms positions found in the XFEL structure can be explained assuming the low oxidation paradigm i.e. Mn1(III)Mn2(IV)Mn3(III)Mn4(II) and a different protonation pattern resulting into different tautomeric forms of the OEC cluster [21]. Such hyphothesis are still matter of debate [22].

In this work we want to verify whether the discrepancies found

[a] *Institute of Chemical Sciences and Engineering, École polytechnique fédérale de Lausanne, Av. F.-A. Forel 2, 1015 Lausanne, Switzerland; E-mail: daniele.narzi@epfl.ch*

[b] *Istituto di Struttura della Materia del Consiglio Nazionale delle Ricerche. Via Salaria, Km. 29,300 - 00016 Monterotondo (RM), Italy; E-mail: giuseppe.mattioli@ism.cnr.it*

[c] *Pangea Formazione s.r.l., via Gaspare Gozzi, 55, Rome, Italy*

[d] *Dipartimento di Scienze Fisiche e Chimiche, Università degli studi dell'Aquila, Via Vetoio (Coppito), 67100 L'Aquila, Italy; E-mail: leonardo.guidoni@univaq.it*

‡ These authors contributed equally to this work

* to whom the correspondence should be addressed

between the XFEL structure and the *ab initio* calculations can be attributed to the presence of different isomers, e.g., an open-cubane and a closed-cubane structure, as already proposed in the case of the S_2 state[23,24] and S_3 state[25–28].

In order to shed light on such hypothesis and to get rid of contradictions, we have first carried out in a QM/MM framework the dynamics of the two most accepted structures for the S_1 state[16,17,19]. Such models share an open-cubane geometry with the W2 molecule present either as H_2O or OH group. Then, we have refined the structure of different S_1 isomers by means of static DFT calculations, by exploring the possibilities of open- and closed-cubane conformations, whose hints were found in the QM/MM results, as well as of both the protonation states investigated for the W_2 water molecule. The putative S_0 state was finally characterized assuming the presence of a proton bound to the μ-oxo O5.

The *ab initio* QM/MM MD simulations of the two S_1 open-cubane models, presenting the W2 water molecule either in the OH or H_2O state (namely S_1^o - W(OH) and S_1^o - W(H_2O) states), have been carried out using the CP2K package[29,30]. Two MD simulations of 17 ps each have been performed, at constant temperature (T = 298 K) by using a setup already applied in the study of the PSII[31–33]. The initial structures of the two simulations have been extracted from the equlibrated QM/MM MD trajectories of the S_2 state[34] properly rearranged following the oxidation and spin states suggested elsewhere[17]. The QM region, consisting of ∼210 atoms, has been treated at DFT+U level (for additional details see Supporting Information). The average intramolecular distances of the manganese cluster and the corresponding standard deviations calculated along the two QM/MM simulations are shown in Tab. 1.

The distribution of the Mn-Mn distances, reported in the top panel of Fig. 2 for both the QM/MM MD simulations, turn out to be almost independent of the protonation state of the water molecule W2, with only minor differences for the Mn1-Mn3 and Mn1-Mn4 distances, slightly increased when W2 is in the H_2O state.

As expected, when W2 is present as H_2O, the Mn4-W1 and Mn4-W2 distances converge towards closer values, passing from 2.37 Å and 1.91 Å in the S_1^o - W(OH) model to 2.19 Å and 2.04 Å in the S_1^o - W(H_2O), in better agreement with the XFEL values (2.25 Å and 2.10 Å respectively). Moreover, the presence of W2 as H_2O affects the Mn1-O5 and Mn4-O5 distances which shift from 2.70 Å and 2.08 Å in the S_1^o - W(OH) model to 2.88 Å and 2.00 Å in the S_1^o - W(H_2O) model. However, even if the S_1-W(OH) model is in this case closer to the XFEL structure, none of the models can be considered as closely compatible with XFEL data (Mn1-O5=2.70 Å and Mn4-O5 = 2.33 Å). Finally, the Mn3-O5 distance (∼1.80 Å in both the simulated models) was found to be considerably far from the corresponding XFEL value (2.20 Å) independently on the protonation state of W2. The spin populations of the four Mn ions in the two models have been also checked along the simulation length (see Fig. 2, bottom panels). In both cases they turn out to be constant along 17 ps of equilibrated dynamics, and in perfect agreement with the oxidation and spin states suggested in Ref.[17], i.e. Mn1(III,↑), Mn2(IV,↓), Mn3(IV,↑), Mn4(III,↓). Overall, our simulations show that both models are stable along the simulation time, albeit they cannot reproduce the O5-Mn3, O5-Mn1 and O5-Mn4 XFEL distances.

Aware of the previous suggestion concerning the O5 position in the XFEL measurements possibly masked by the presence of the three neighboring Mn atoms[14], we tried to spotlight the apparent contradiction regarding such position by means of static DFT simulations of different configurations (see Fig. 1), performed by using the ORCA package in a similar setup employed in Ref.[35] and reported in details in Supporting Information. We note first that previously calculated S_1 models[16,19] are characterized by an open-cubane configuration with O5 close to Mn4 and Mn3, far from Mn1 and holding a substantially twofold-coordinated Mn-O-Mn position. If it was the only stable configuration of S_1, not masked by the far Mn1 atom, we could expect a closer agreement between XFEL results and single DFT configurations, similar to that found in the case of the Mn-O distances involving the twofold- and threefold-coordinated O1-O4 atoms (see Table 1 for comparison). which can be indicative S_1 state. Indeed, we found two stable isomers of S_1, having an open-cubane and a closed-cubane structure, respectively, in the case of both protonation patterns of W2, as depicted in Fig. 1 (a-d).

Selected intramolecular distances of the Mn_4CaO_5 cluster in such four models (namely S_1^o - W(OH), S_1^o - W(H_2O), S_1^c - W(OH) and S_1^c - W(H_2O)) are reported in Tab. 1 (see also Tab.S1 for the full set of distances). As a general trend open models are closer to the XFEL structure than closed models independently of the protonation state of W2, with some noteworthy exception. For example, Mn1-Mn3 is longer in open models and closer to the XFEL value than in closed models. On the contrary, Mn3-Mn4 is longer in the closed than in the open models, with the XFEL value falling between the two sets of calculated distances. A similar situation is also found in the case of Mn1-Ca, with the XFEL value almost equidistant from the two configurations.

The protonation state of W2 affects the distances between Mn4 and the two bound water molecules W1 and W2. In particular Mn4-W2 is shorter, as expected, in the case of W2(OH) (∼1.9 Å), and longer and in better agreement with XFEL in the case of W2(H_2O) (∼2.0 Å), irrespective of the open-/closed-cubane configuration. Mn4-W1 is instead slightly sensitive to the protonation of W2. Finally, key distances involving O5 deserve a focused close-up. Mn1-O5 is longer than XFEL (2.70 Å) in open models (2.92 Å for W2(OH) and 3.06 Å for W2(H_2O)), and considerably shorter in closed models (2.11 Å for W2(OH) and 2.14 Å for W2(H_2O)). The opposite holds in the case of Mn4-O5, where the distance is longer than XFEL (2.33 Å) in the case of closed models (2.93 Å for W2(OH) and 2.74 Å for W2(H_2O)), and shorter in the case of open models (1.94 Å for W2(OH) and 1.89 Å for W2(H_2O)). This situation is clearly compatible with a mixing of open and closed structures in the measured sample. As mentioned above, it should be also noted that Mn3-O5 (∼1.8 Å in all models) is basically insensitive to the open-closed motif and to the protonation of W2, and systematically shorter than the XFEL value (2.20 Å). This supports the suggestion that the XFEL sample was contaminated by a minority fraction of S_0, in which O5 is expected to be protonated and, therefore, compatible with a longer

Mn3-O5 distance.

Overall, the four investigated S_1 models are characterized by root mean square deviations (rmsd) close to ∼0.2 Å with respect to the XFEL values (see Tab.S2). Nevertheless, the combination of the two open and closed cubane isomers leads to a best rmsd of ∼0.17 and ∼0.16 Å depending on the W2 state, with a slightly higher contribution of the open cubane isomers. This allows an optimal average displacement of O5, with Mn1-O5 and Mn4-O5 very close to the XFEL values (see Tab.S3). The Mn-Mn distances found in our combined models show three values (i.e. Mn1-Mn2, Mn2-Mn3 and Mn3-Mn4) between 2.74 and 2.85 Å and a higher value (Mn1-Mn3) ∼3.15 Å (see mixed structures ac and bd in Tab.S3) in good agreement with XAFS data[36,37]. Additionally, in XAFS experiments one of the three short Mn-Mn distances turns out to be longer than the others. Intriguingly, the Mn3-Mn4 distance found in our S_1 models depends largely on the given isomer (∼ 2.7 Å in S_1^o and ∼ 3.0 Å in S_1^c). In this respect, the presence of a fraction of the closed cubane isomer in the S_1 state could explain the larger value of one of the three distances, namely the Mn3-Mn4, found in both XFEL and XAFS data. These results provide a sound indication of the presence of two nearly isoenergetic isomers consistent with the S_1 state, as already suggested for the S_2[23,24] and the S_3 states[25–28]. Indeed, we have calculated an energy difference of ∼0.09 kcal/mol for the two isomers in their broken symmetry ground state with the open-cubane structure *b* more stable than the closed-cubane structure *d* (see the Supporting Information for details). The energy difference is lower than that found by Isobe et al. (∼8 kcal/mol)[38] by using a significantly smaller portion of the PSII core.

Recent room-temperature EXAFS measurements seem to exclude the fast interconversion of S_1 isomers[39], whereas diffraction measurements carried out with an extremely low radiation dose produce results similar to XFEL and support the occurrence of isomers in the damage-free PSII dark state[40]. Such results are compatible with the presence of stable structures characterized by a low interconversion dynamics (due, e.g., to a barrier higher than that calculated in the case of S_2[24]), as well as with an S_0 contamination of the XFEL sample.

QM calculations characterizing the possible S_0 state (results shown in Tab.S1) have been additionally carried out considering two models differing only for the protonation state of W2 and both presenting a protonated O5 μ-oxo (details of such models can be found in Supporting Information). Combining the optimized structures of the two open and closed cubane S_1 isomers with a minority (∼30%) contribution of the optimized S_0 models we obtained best rmsd values of 0.167 Å for the models presenting W2 as hydroxyl group and 0.153 Å for the models with W2 as H_2O (see Tab.S2) with a Mn3-O5 distance closer to the XFEL value (see Tab.S3). Our results suggest the presence of two isomers consistent with the S_1 state, possibly presenting the W2 water in the H_2O form, and an appreciable amount of S_0 state in the PSII crystals measured by the XFEL experiment. The presence of such isomers, structuraly analogue to those present in the S_2 state and nearly isoenergetic, can reconcile XFEL data with those obtained by theoretical studies.

References

1 J. P. McEvoy and G. W. Brudvig, *Chem. Rev.*, 2006, **106**, 4455–4483.
2 B. Kok, B. Forbush and M. McGloin, *Photochem. Photobiol.*, 1970, **11**, 457–475.
3 P. Joliot and B. Kok, *Bioenergetics of Photosynthesis*, 1975, 387–412.
4 M. W. Kanan and D. G. Nocera, *Science*, 2008, **321**, 1072–1075.
5 J. Barber, *Chem. Soc. Rev.*, 2009, **38**, 185–196.
6 T. Faunce, S. Styring, M. R. Wasielewski, G. W. Brudvig, A. W. Rutherford, J. Messinger, A. F. Lee, C. L. Hill, H. deGroot, M. Fontecave, D. R. MacFarlane, B. Hankamer, D. G. Nocera, D. M. Tiede, H. Dau, W. Hillier, L. Wang and R. Amal, *Energy Envir. Sci.*, 2013, **6**, 1074–1076.
7 A. Zouni, H. T. Witt, J. Kern, P. Fromme, N. Krauss, W. Saenger and P. Orth, *Nature*, 2001, **409**, 739–743.
8 K. N. Ferreira, T. M. Iverson, K. Maghlaoui, J. Barber and S. Iwata, *Science*, 2004, **303**, 1831–1838.
9 B. Loll, J. Kern, W. Saenger, A. Zouni and B. J, *Nature*, 2005, **438**, 1040–1044.
10 H. Dau, A. Grundmeier, P. Loja and M. Haumann, *Phil. Trans. Royal Soc. B - Biol. Sci.*, 2008, **363**, 1237–1243.
11 A. Guskov, J. Kern, A. Gabdulkhakov, M. Broser, A. Zouni and S. W, *Nat. Struct. Mol. Biol.*, 2009, **16**, 334–342.
12 Y. Umena, K. Kawakami, J.-R. Shen and N. Kamiya, *Nature*, 2011, **473**, 55–60.
13 M. Suga, F. Akita, K. Hirata, G. Ueno, H. Murakami, Y. Nakajima, T. Shimizu, K. Yamashita, M. Yamamoto, H. Ago and J. R. Shen, *Nature*, 2015, **517**, 99–103.
14 M. Askerka, D. J. Vinyard, J. Wang, G. W. Brudvig and V. S. Batista, *Biochemistry*, 2015, **54**, 1713–1716.
15 P. Chernev, I. Zaharieva, E. Rossini, A. Galstyan, H. Dau and E. Knapp, *J. Phys. Chem. B*, 2016, **120**, 10899–10922.
16 P. E. M. Siegbahn, *Biochim. Biophys. Acta -Bioenergetics*, 2013, **1827**, 1003–1019.
17 V. Krewald, M. Retegan, N. Cox, J. Messinger, W. Lubitz, S. DeBeer, F. Neese and D. A. Pantazis, *Chem. Sci.*, 2015, **6**, 1676–1695.
18 A. Klauss, M. Haumann and H. Dau, *Proc. Natl. Acad. Sci. USA*, 2012, **109**, 16035–16040.
19 S. Luber, I. Rivalta, Y. Umena, K. Kawakami, J.-R. Shen, N. Kamiya, G. W. Brudvig and V. S. Batista, *Biochemistry*, 2011, **50**, 6308–6311.
20 V. Krewald, M. Retegan, F. Neese, W. Lubitz and N. Pantazis D A, and Cox, *Inorg. Chem.*, 2016, **55**, 488–501.
21 S. Petrie, R. J. Pace and R. Stranger, *Angew. Chem. Int. Ed.*, 2015, **54**, 7120–7124.
22 K. M. Davis, M. C. Palenik, L. Yan, P. F. Smith, G. T. Seidler, C. Dismukes and Y. N. Pushkar, *J. Phys. Chem. C*, 2016, **120**, 3326–3333.
23 D. A. Pantazis, W. Ames, N. Cox, W. Lubitz and F. Neese, *Angew. Chem. Int. Ed.*, 2012, **51**, 9935–9940.
24 D. Bovi, D. Narzi and L. Guidoni, *Angew. Chem. Int. Ed.*, 2013, **52**, 11744–11749.
25 M. Capone, D. Bovi, D. Narzi and L. Guidoni, *Biochemistry*, 2015, **54**, 6439–6442.
26 M. Askerka, J. Wang, D. J. Vinyard, G. W. Brudvig and V. S. Batista, *Biochemistry*, 2016, **55**, 981–984.
27 M. Retegan, V. Krewald, F. Mamedov, F. Neese, W. Lubitz, N. Cox and D. Pantazis, *Chem. Sci.*, 2016, **7**, 72–84.
28 M. Capone, D. Narzi, D. Bovi and L. Guidoni, *J. Phys. Chem. Lett.*, 2016, **7**, 592–596.
29 T. Laino, F. Mohamed, A. Laio and M. Parrinello, *J. Chem. Theory Comput.*, 2005, **1**, 1176–1184.
30 J. VandeVondele, M. Krack, F. Mohamed, M. Parrinello, T. Chassaing and J. Hutter, *Comput. Phys. Comm.*, 2005, **167**, 103–128.
31 D. Narzi, D. Bovi and L. Guidoni, *Proc. Natl. Acad. Sci. USA*, 2014, **111**, 8723–8728.
32 F. Pitari, D. Bovi, D. Narzi and L. Guidoni, *Biochemistry*, 2015, **54**, 5959–5968.
33 D. Narzi, D. Bovi, P. De Gaetano and L. Guidoni, *J. Am. Chem. Soc.*, 2016, **138**, 257–264.
34 D. Bovi, D. Narzi and L. Guidoni, *New J. Phys.*, 2014, **16**, 015020.
35 W. Ames, D. A. Pantazis, V. Krewald, N. Cox, J. Messinger, W. Lubitz and F. Neese, *J. Am. Chem. Soc.*, 2011, **133**, 19743–19757.
36 A. Grundmeier and H. Dau, *Biochim. Biophys. Acta -Bioenergetics*, 2012, **1817**, 88–105.
37 C. Glöckner, J. Kern, M. Broser, A. Zouni, V. Yachandra and J. Yano, *J. Biol. Chem.*, 2013, **288**, 22607–22620.
38 H. Isobe, M. Shoji, S. Yamanaka, Y. Umena, K. Kawakami, N. Kamiya, J. Shen and K. Yamaguchi, *Dalton Trans.*, 2012, **41**, 13727–13740.
39 K. M. Davis and Y. N. Pushkar, *J. Phys. Chem. B*, 2015, **119**, 3492–3498.
40 A. Tanaka, Y. Fukushima and N. Kamiya, *J. Am. Chem. Soc.*, 2017, **139**, 1718–1721.

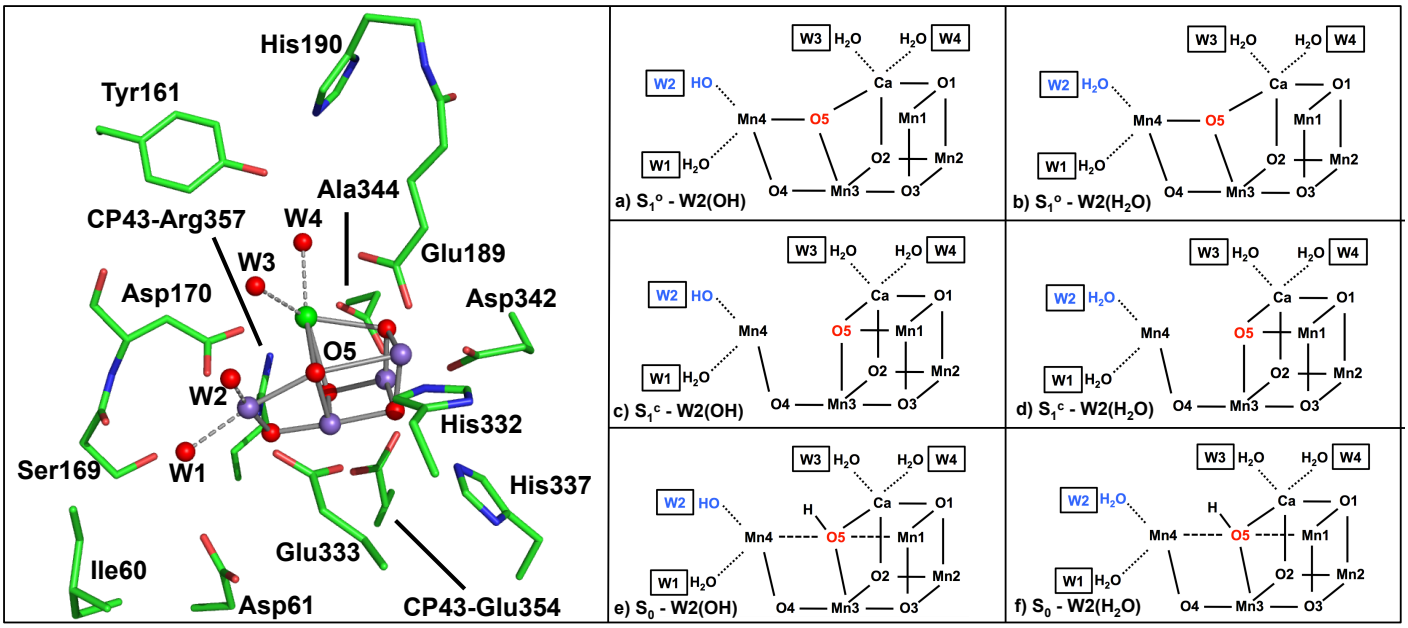


Fig. 1 Left panel: Quantum Mechanical model of the Mn_4CaO_5 cluster in PSII. The water molecules not directly bound to the Mn_4CaO_5 cluster have been omitted for the sake of clarity. Right panel: Representative schemes of the models investigated in this study. Four S_1 states (two open and two closed cubane models with two forms of the W2 water molecule and two S_0 states with two forms of W2). O5 and W2 (OH or H_2O) are highlighted in red and blue respectively.

Table 1 Comparison of the main distances [Å] in the Mn_4CaO_5 cluster between the XFEL structure and the S_1 state in the QM/MM description (values averaged over 17 ps of simulation MD, standard deviations shown in brackets) and in the full QM description.

	QM/MM MD simulations		Static QM calculations				
	S_1^o - W(OH)	S_1^o - W(H_2O)	S_1^o - W(OH)	S_1^o - W(H_2O)	S_1^c - W(OH)	S_1^c - W(H_2O)	XFEL
Mn1-Mn2	2.79 (0.06)	2.77 (0.06)	2.76	2.77	2.72	2.73	2.68
Mn1-Mn3	3.22 (0.12)	3.29 (0.12)	3.23	3.31	2.98	2.97	3.20
Mn1-Mn4	4.76 (0.18)	4.85 (0.16)	4.84	4.91	4.99	4.85	4.95
Mn2-Mn3	2.80 (0.07)	2.80 (0.06)	2.79	2.78	2.78	2.77	2.70
Mn3-Mn4	2.78 (0.07)	2.76 (0.06)	2.73	2.70	3.07	2.97	2.87
Mn1-Ca	3.54 (0.12)	3.57 (0.14)	3.56	3.59	3.37	3.33	3.47
Mn2-Ca	3.41 (0.11)	3.33 (0.10)	3.33	3.33	3.37	3.35	3.32
Mn3-Ca	3.51 (0.13)	3.44 (0.11)	3.40	3.44	3.29	3.29	3.40
Mn4-Ca	3.67 (0.14)	3.66 (0.13)	3.69	3.71	4.03	3.93	3.77
Mn4-W1	2.37 (0.23)	2.19 (0.16)	2.09	2.06	2.15	2.17	2.25
Mn4-W2	1.91 (0.05)	2.04 (0.08)	1.89	2.01	1.89	1.98	2.10
Mn1-O1	1.88 (0.05)	1.86 (0.04)	1.85	1.85	1.86	1.85	1.80
Mn1-O3	1.94 (0.05)	1.94 (0.06)	1.89	1.91	1.92	1.92	1.87
Mn1-O5	2.70 (0.23)	2.88 (0.22)	2.92	3.06	2.10	2.14	2.70
Mn2-O1	1.86 (0.05)	1.84 (0.05)	1.87	1.87	1.84	1.84	1.82
Mn2-O2	1.82 (0.05)	1.83 (0.05)	1.80	1.80	1.83	1.83	1.83
Mn2-O3	1.91 (0.05)	1.91 (0.05)	1.89	1.89	1.86	1.86	2.02
Mn3-O2	1.87 (0.06)	1.87 (0.05)	1.87	1.87	1.87	1.87	1.90
Mn3-O3	2.03 (0.07)	2.04 (0.08)	2.04	2.03	2.01	2.00	2.06
Mn3-O4	1.82 (0.05)	1.84 (0.05)	1.79	1.81	1.79	1.81	1.90
Mn3-O5	1.80 (0.05)	1.81 (0.05)	1.80	1.81	1.82	1.80	2.20
Mn4-O4	1.88 (0.05)	1.86 (0.06)	1.86	1.82	1.85	1.81	2.02
Mn4-O5	2.08 (0.15)	2.00 (0.12)	1.94	1.89	2.93	2.74	2.33

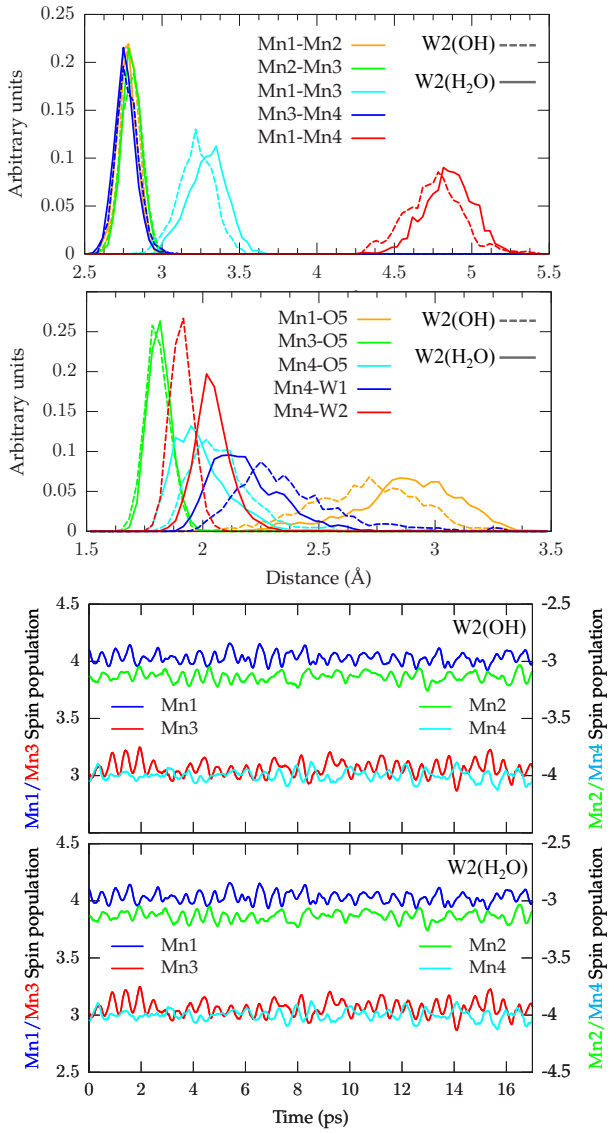


Fig. 2 Distribution of selected distances in the Mn_4CaO_5 cluster (two top panels) and time evolution of the spin populations of the Mn ions (two bottom panels) calculated along the two QM/MM MD simulations.